



Research Article

Analysis of Electrical Characteristics of Composite Insulators with the Presence of Optimum Layer of ZnO Microvaristors

Milad Darmiani ¹, Reza Shariatinasab,¹ Hamidreza Najafi,¹ Morteza Ghayedi ¹
and Eduardo M. G. Rodrigues ^{2,3}

¹Department of Electrical and Computer Engineering, University of Birjand, Birjand, Iran

²Department of Electrical and Computer Engineering, Instituto Superior Técnico, Lisboa, Portugal

³INESC-ID, Sustainable Power Systems Group, Instituto Superior Técnico, Universidade de Lisboa, 1049-001, Lisboa, Portugal

Correspondence should be addressed to Morteza Ghayedi; m.ghayedi@birjand.ac.ir
and Eduardo M. G. Rodrigues; eduardo.g.rodrigues@tecnico.ulisboa.pt

Received 17 November 2022; Revised 9 April 2023; Accepted 14 June 2023; Published 29 July 2023

Academic Editor: Samarjeet Singh Siwal

Copyright © 2023 Milad Darmiani et al. This is an open access article distributed under the Creative Commons Attribution License, which permits unrestricted use, distribution, and reproduction in any medium, provided the original work is properly cited.

The electric field distribution of insulator surface is nonuniform, and the maximum electric field is visible around two terminals of the insulator. Using a microvaristor layer is one of the methods of field control that can reduce the electric field stresses to prevent an extension of discharges on the insulator surface and a complete flashover caused by the subsequent development of arcing. This study targets the effect of zinc oxide (ZnO) microvaristors on the electric field distribution along the contaminated and clean composite insulators that have been investigated. In addition, the impact of the insertion of microvaristor layers on the critical flashover voltage (CFO) of the insulators through a mathematical formula has been presented for the first time. The estimation of electric field distribution is conducted through finite element method (FEM) on a 400 kV insulator using COMSOL Multiphysics, in which the optimal dimensions of the microvaristor layer were obtained using the accelerated particle swarm optimization (APSO) algorithm. Then, for the first time, the analysis of the influence of the ZnO insertion on the transient performance of the insulator, i.e., the outage rate of the network, is performed in EMTP software for the insulator with the optimized insertion of the microvaristor layer. Modelling techniques were used to simulate the components of a transmission network according to the valid models. Finally, by setting different values for CFO, Monte Carlo simulation, and linking EMTP and MATLAB software, the lightning flashover rate (LFOR) and the failure risk (F.R.) of the different insulator models are calculated. It is shown that the proposed method reduces the maximum electric field of the inside and outside of the insulator, which in turn leads to a reduction in the outage rate of the power network and the insulation risk of the insulator, and an increase in CFO of the insulator.

1. Introduction

Quick advancements in power network insulation have persuaded power utilities to replace composite insulators with old ones. Compared to traditional porcelain and glass insulators, composite insulators are superior in breakage resistance, lightness, performance in pollution, and so on [1–3]. However, composite insulators are subject to electrical, mechanical, and environmental stresses. Both normal and transient conditions arose by switching operation and lightning strokes lead to the electrical stress in composite insula-

tors [4]. The electrical stress is vital in the presence of a strong field around the electrodes, i.e., the high voltage (HV) and the ground terminals of the insulator [5–7]. Extension of discharges on the insulator surface and the following development of arcing imposed by the high electric field may finally cause an insulation failure or a complete flashover [8].

Since field magnitudes around the terminals of insulators are higher than the middle sections, reducing the electric field in vicinity of the terminals is effective for better performance of the insulators [5]. In other words, uniform

the electric field distribution and decrement of the electric field in improving CFO of the insulator. In recent years, using the technology has developed the meaning of electric stress control. Applications of microvaristor for electrical machines and transmission lines and their performance improvement have been presented in [9, 10]. In research [4], improvement due to the microvaristor layer reported a 21% increase in flashover voltage in breakdown tests.

ZnO microvaristor as a semiconductor with a large direct band gap (3.37 eV) and high binding energy of 60 meV at room temperature as semiconductor material [11] is widely applied in the area of high voltage [12]. For example, introducing nanoparticles such as ZnO into transformer oils brings out some merits including improved partial discharge properties; better AC, DC, and impulse breakdown performances; better performance of transformer cooling; making less sensitive to moisture; and increased thermal conductivity [13]. Duzkaya and Beroual [14] showed that natural ester-based nanofluids with ZnO nanoparticles as semiconductive can make the AC breakdown performance better. Recently, Xie et al. [15] reveal that the SiR/ZnO composites have a significant smoothing effect on nonuniform AC electrical field at the tip and suppress corona discharge. In [16], by using ZnO varistor as a material with nonlinear conductivity, the electric field in the cable terminal accessory was diminished.

The microvaristor conductivity increases above a threshold field domain, and hence, it can be applied to decrease the maximum electric field experienced at critical sections of the insulator [17]. The use of a microvaristor layer with two different thicknesses in a composite insulator with FEM modelling and laboratory test has been presented in [18] in which the results demonstrate the effectiveness of the microvaristor in decreasing the electric field intensity in the regions near to the insulator terminals. Also, the investigations on the effect of a thin layer of microvaristor on polluted and clean composite insulators are available in [19], and the results showed a significant decrement in field magnitude on the insulator surface. Recently, authors in [20] applied nonlinear composites as the field grading material (FGM) in polymeric outdoor insulators and obtained the simulations and experimental results. Applying nonlinear field-dependent conductivity to reduce the high electric field issue in an envisaged 25 kV high-density wide bandgap power module was proposed by authors in [21].

So far, electric field control has been achieved utilizing microvaristors; however, the following issues arise in this literature: (a) How does the microvaristor layer affect the failure risk of insulators and LFOR of the power network? (b) How could a mathematical expression represent the impact of a microvaristor on CFO which indeed can result in the network outage rate? (c) How to calculate the costs related to the improvement of the insulator dielectric strength? In accordance with the above-discussed literature, this paper is aimed at addressing these concerns and the research gap for the first time to the best of our knowledge. To this aim, the proposed insulator model is simulated by the EMTP package, and the CFO value of the model is determined by a new mathematic formulation. In this study, a suitable loca-

tion where the microvaristor layer must be inserted into the housing of the composite insulator is determined so that the electric field along the insulator is minimized. In order to go through this, the electric field distribution is obtained from FEM using COMSOL software. The microvaristor dimension is optimized by connecting MATLAB to COMSOL and the use of APSO algorithm for transient analysis. Also, regarding the probabilistic nature of the lightning wave, Monte Carlo method is introduced to calculate the values of CFO updated with the link between EMTP and MATLAB. The contributions of this study can be briefly summarized as follows: proposing a new mathematical formulation taking into account the variations of the electric field distribution caused by the presence of microvaristors in order to calculate the insulator's the CFO value; performing an optimal strategy via a link between COMSOL and MATLAB software; employment of microvaristors potential for analyzing the failure risk of insulators and LFOR of the network caused by insulators with microvaristors through a link between EMTP and MATLAB.

2. Finite Element Modelling

2.1. Simulation of Insulator. In this research, FEM investigation is done by applying the electrostatic (es) module in COMSOL Multiphysics.

Composite insulators commonly comprise four main components: (i) fiber-reinforced polymer (FRP) rod; (ii) polymer sheath on the rod; (iii) polymer weather sheds; (iv) metal and fitting [22]. The composite insulator is considered as a symmetric 400 kV insulator, so an axisymmetric model is used to simulate the insulator (Figure 1).

Simulation dimensions of the 400 kV composite insulator used in this paper according to [23] are detailed in Table 1.

The microvaristor applied in this simulation exhibits an extremely nonlinear characteristic (see Figure 2).

As can be depicted in Figure 2, if the applied field oversteps the field threshold, the conductivity of the microvaristor increases and enters the conduction region. Also, to model the contamination, an unchangeable layer with a 0.5 mm width is assumed on the surface of the insulator, while its conductivity is set to 6×10^{-7} S/m, and its relative permittivity of 80 is used [24].

The geometry and electrical properties of materials used in the proposed insulator are indicated in Figure 3 and Table 2, respectively.

In this study, by changing the place of microvaristor injection, its impact on the maximum field has been investigated. Five different modes of insulators with their various injection places have been demonstrated in Figure 4.

2.2. Finite Element Analysis. The finite element analysis is an acceptable numerical method for analyzing many problems of physics and engineering [25–27]. Using a variety of mathematical theorems, a discrete differential equation with given conditions for the electric field, FEM produces a linear/non-linear system of equations that should be solved. FEM proceeds from the following step to build and solve the

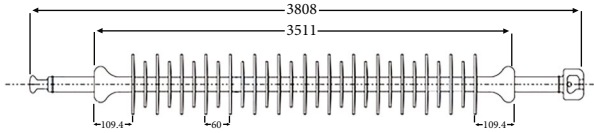


FIGURE 1: Geometry and profile of insulator.

TABLE 1: Geometric parameters of insulator.

Dimensions	Value (mm)
Small shed diameter	110
Large shed diameter	145
Shed spacing	30
Total length	3808
Arcing distance	3560

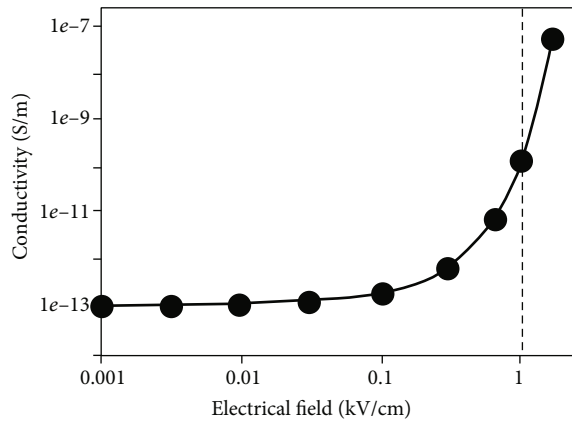


FIGURE 2: Characteristic of the microvaristor [6].

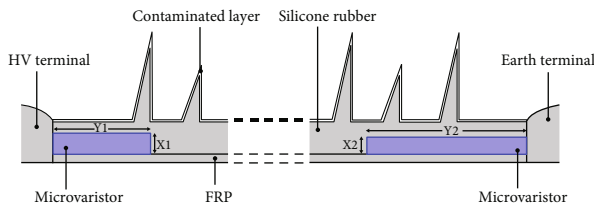


FIGURE 3: Proposed insulator model.

TABLE 2: Material properties of insulator [4].

Materials	Relative permittivity (ϵ_r)	Conductivity (σ (S/m))
Silicone rubber	4.3	1×10^{-13}
Forged steel	1	5.9×10^7
Air	1	1×10^{-13}
Microvaristor	12	σ (E)
FRP	7.1	1×10^{-13}

equations to calculate electric fields: step 1: definition of the insulator geometry; step 2: meshing of the geometry; step 3: determination of material type; step 4: definition of boundary conditions; step 5: electric field computation on the insulator profile. To calculate the electric potential and field on

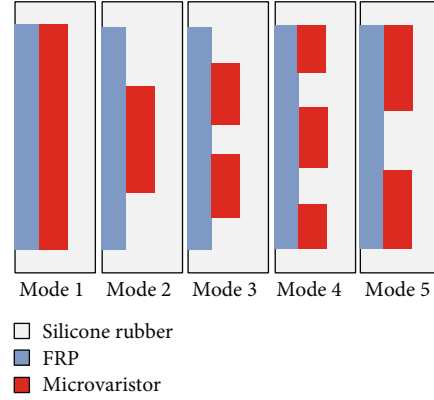


FIGURE 4: Different injections of microvaristor in insulator structure.

the insulator surface, the electrostatic form of the Maxwell's equation [28] is solved, and to compute the electric potential, the electric field of the insulator surface should be calculated (see [29] for further details).

2.3. Modelling Results. Using the existing governing equations, five different insulator modes are simulated in COM-SOL environment.

In this paper, the effect of microvaristor layer presence on the maximum field and dissipated power of different insulator models (Figure 4) is investigated, and its results are shown in Table 3. Also, based on the relations in [4], the dissipated power is calculated in the volume unit of the insulator (P_V).

Regarding the results presented in Table 3, it can be seen that the injection of the microvaristor layer has a positive effect on reducing the maximum field of the insulator surface and dissipated power of all models. Based on the maximum field and dissipated power values in Table 3, the worst and the best modes are seen in 3rd and 5th insulator modes, respectively. Also, comparing 1st and 5th mode results, it is clear that the injection of a large amount of microvaristor does not necessarily lead to better results.

By considering the high electric field density in the vicinity of the insulator terminals and Table 3, mode 5 is selected as the proposed model of insulator. Therefore, the microvaristor is placed between the core and silicone housing of the insulator in the vicinity of the insulator terminals.

Figures 5 and 6 show the equipotential contours around the HV terminal for the insulator model without and with microvaristor, respectively. As can be observed from these figures, the density of the equipotential contours at two terminals in the insulator without microvaristor is higher than the insulator with microvaristor. Also, the displacement of the equipotential line from two terminals of the insulator to central sections of the insulator can be seen in Figure 6; thus, the reason for reduction in the electric field near the terminals is the displacement of contours that leads to a decrease in the gradient.

3. Optimization

The optimal dimensions of the injected microvaristors are necessary to obtain the lowest electric field accumulation.

TABLE 3: Maximum field and P_V of different insulator models.

Insulator models	E_{\max} (kV/cm)	P_V (W/cm ³)
Without microvaristor	45.29	12.30
Mode 1 with microvaristor	42.17	10.67
Mode 2 with microvaristor	43.57	11.38
Mode 3 with microvaristor	43.63	11.42
Mode 4 with microvaristor	42.33	10.75
Mode 5 with microvaristor	41.84	10.50

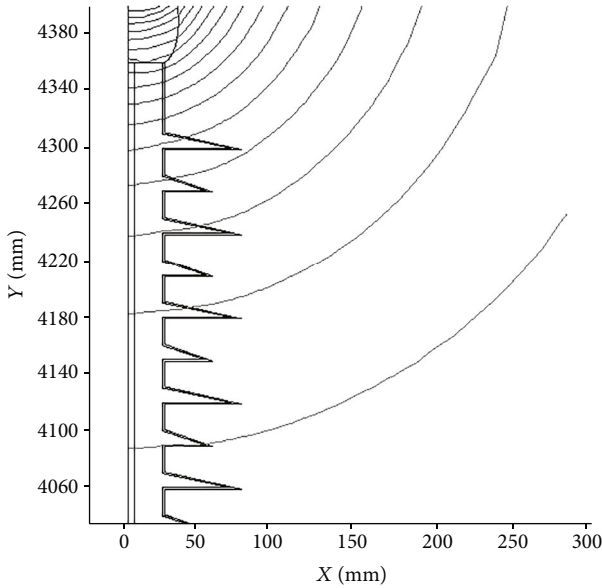


FIGURE 5: Electric potential lines of insulator without microvaristor.

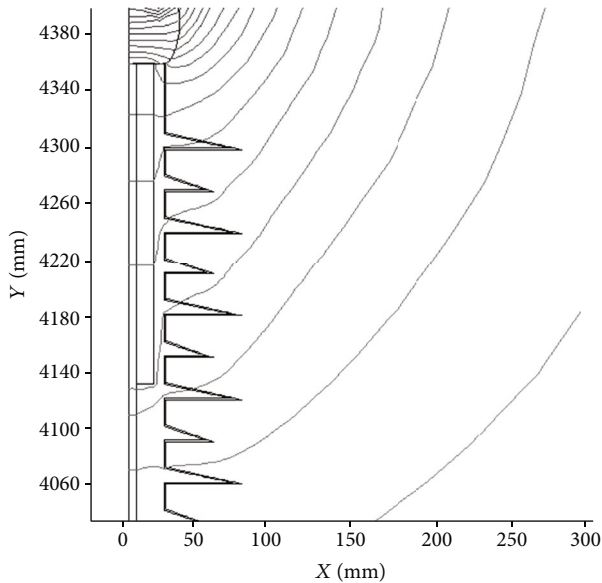


FIGURE 6: Electric potential lines of insulator with microvaristor.

Hence, because of the hugeness of problem space, the evolutionary algorithm is needed. One of the useful intelligent algorithms for resolving the designing problem of high-voltage equipment is APSO optimization algorithm. APSO

algorithm is a simplified version of the standard PSO which can speed up the convergence due to the use of the global best. The general steps of the optimization process adopted from [30, 31] are as follows:

- Step 1: generating the initial population
- Step 2: computing and evaluating the objective function
- Step 3: creating the new population
- Step 4: investigating constraints
- Step 5: selection
- Step 6: going to step 3 and repeating until the convergence criterion is met

The optimization of microvaristor layers in order to improve the maximum field is done by establishing a link between COMSOL and MATLAB software. In fact, the insulator with ZnO microvaristor layers is simulated in COMSOL to calculate the maximum field. Then, the obtained results are transmitted to MATLAB in order to evaluate the objective function.

3.1. Objective Function. The purpose of the optimization algorithm is to minimize the maximum electric field density (E_{\max}) of insulator with injecting microvaristor. Therefore, function is described as follows:

$$\text{Objective function} = \text{Min} (E_{\max}). \quad (1)$$

The width and height of the injected microvaristor layers are the optimization variables; in this way, X_1 and Y_1 are the width and height of the injected microvaristor layer in the vicinity of the HV terminal, respectively (see Figure 3). Also, X_2 and Y_2 are the width and height of the microvaristor layer near the earth terminal, respectively.

The flowchart of the used algorithm is shown in Figure 7.

3.2. Results of Optimization. Table 4 presents the maximum value of the electric field, the ratio of the maximum field to the average field of the insulator (Schwaiger factor), and the dissipated power before and after optimization.

By comparing the results shown in Table 4, it can be realized that the presence of microvaristor layers reduces the maximum field and moreover provides a more uniform field on the surface of the insulator than the insulator without microvaristor layers. As can be seen in the table, the results show a 13.3% decrease in the maximum field and a 20.7% decrease in the Schwaiger factor when ZnO microvaristor-optimized layers are injected into the structure of the insulator.

Also, it can be seen that the dissipated power (P_V) is decreased by 25% nearly, which indicates a reduction in the temperature and heat at the insulator surface.

In this work, also the effectiveness of microvaristor layers on the insulator under clean surface conditions has been investigated, and its results can be seen in Table 5.

According to Table 5, the maximum electric field of the insulator with ZnO microvaristor has been reduced from 37.10 kV/cm to 32.86 kV/cm.

The field distribution of the insulator with and without ZnO microvaristor under contaminated surface conditions is plotted in Figure 8.

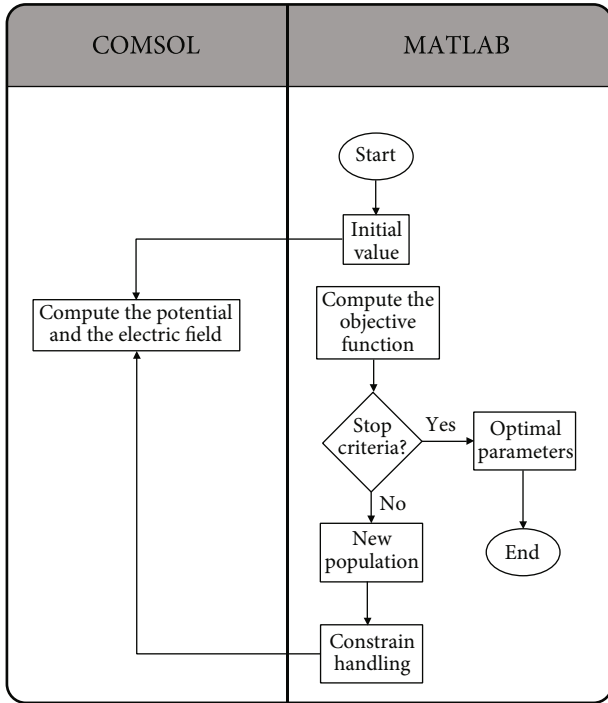


FIGURE 7: Electric optimization flowchart of microvaristor layers.

As can be observed in Figure 8, with the approach used in this study, in addition to the reduction of the electric field near the terminals, the field distribution on the insulator surface becomes more uniform correspondingly as the electric field is increased in the central areas of the insulator with ZnO microvaristor. The uniform distribution of the field and maximum reduction of the electric field lead to the reduction of the surface discharge probability on the insulator surface and improve the performance of the insulator.

4. EMTP Modelling

To figure out the effect of microvaristor layer injection on the network outage rate, the optimized insulator should be properly modelled in EMTP.

To calculate the variation of CFO, the program needs to use one of the outputs of COMSOL Multiphysics. This is while the electric field is one of the main results. Hence, an approach is necessary to present a link between the electric field and the mentioned index. It is clear that E_{mean} in uniform fields can be expressed as

$$E_{\text{mean}} = \frac{V_{\text{applied}}}{d}, \quad (2)$$

where V_{applied} and d are applied voltage and distance between two electrodes, respectively. According to [32], the ‘‘Schwaiger factor’’ η as the efficiency of the electric field can be defined as follows:

$$\eta = \frac{E_{\text{mean}}}{E_{\text{max}}} = \frac{V_{\text{applied}}}{d E_{\text{max}}}. \quad (3)$$

Since the maximum field intensity of insulator surface is equal to the breakdown of the air ($E_{\text{max}} = E_b$), the above equation can be revised as

$$V_b = \eta d E_b. \quad (4)$$

In the above expression, V_b is the breakdown voltage [32]. After substituting (2) and (3) in (4)

$$V_b = \frac{V_{\text{applied}} \cdot E_b}{E_{\text{max}}}. \quad (5)$$

Equation (5) is particularly beneficial to estimate the CFO of an insulator. Therefore, reducing and controlling the maximum field could be a useful technique to increase the CFO of an insulator. The CFO values, as presented in Table 6, are calculated by using Equation (5) and the obtained results from Tables 4 and 5.

The disruptive effect (DE) model is utilized to determine the effect of the injected ZnO microvaristor layer leading to the variation CFO. Therefore, having CFO, an appropriate DE model, can be simulated in EMTP.

The insulator string can be modelled by [33]:

$$\begin{aligned} E &= \int_{t_0}^t [v(t) - V_0]^k dt, \\ V_0 &= 0.77 \cdot \text{CFO}, \\ \text{DE}_b &= 1.15 \cdot \text{CFO}^{1.36}, \end{aligned} \quad (6)$$

where DE is the criterion to recognize the breakdown event when DE exceeds the critical disruptive effect DE_b , V_0 (kV) is the minimum required voltage where breakdown occurrence starts, and t_0 (μs) is the moment that the instantaneous voltage $v(t)$ is higher than V_0 .

5. Simulation Results

The effect of ZnO microvaristor on the outage rate or LFOR and the failure risk is investigated. These evaluations have been done on a 400 kV transmission line by EMTP-like tool which has the ability to link to MATLAB. The needed parameters to simulate in EMTP are defined as follows.

5.1. Lightning Parameters. The peak current, I_p , rise time, t_f , and tail time, t_h , are the major parameters of the lightning waveforms. Having main parameters of the lightning waveform, the lightning current surge can be proposed by the Heidler function [34]:

$$I(t) = \frac{I_p}{\eta} \frac{k^n}{1 + k^n} e^{-t/\tau_2}, \quad (7)$$

where I_p is the peak value of current, n is the current steepness factor, η is the correction factor of the peak current, and $k = t/\tau_1$ and τ_1 , and τ_2 are time constants for determining the rise and decay time of lightning, respectively.

TABLE 4: Maximum field, E_{\max}/E_{mean} , and dimensions of microvaristor layers.

Parameters	Insulator without microvaristor layers	Insulator with microvaristor-optimized layers
E_{\max} (kV/cm)	45.29	39.26
E_{\max}/E_{mean}	38.49	30.51
P_V (W/cm ³)	12.30	9.24
X_1 (mm)	—	14.20
X_2 (mm)	—	11.38
Y_1 (mm)	—	372.33
Y_2 (mm)	—	361.07

TABLE 5: Maximum field of clean insulator before and after optimization.

Insulator models	E_{\max} (kV/cm)
Without microvaristor layers	37.10
With microvaristor-optimized layers	32.86

5.2. *Tower Footing Impedance.* In this work, the footing impedance is expressed as a nonlinear resistance R_f . It is given by [35]:

$$R_f = \frac{R_0}{\sqrt{1 + (I/I_g)}}, \quad (8)$$

$$I_g = \frac{1}{2\pi} \cdot \frac{\rho E_0}{R_0^2},$$

where R_0 is the footing resistance at low current and low frequency, I is the stroke current through the resistance, I_g is the limiting current to initiate sufficient soil ionization, ρ is the soil resistivity (ohm.m), and E_0 is the soil ionization gradient (400 kV/m).

5.3. *Transmission Tower and Line.* Figure 9 shows the schematic diagram of the tower of the 400 kV test line and its multistory model in this work. The characteristics of the line conductors are shown in Table 7.

In the multistory model, $Zt1$ (= 200 ohm) is assumed as the tower top to the phase arm impedance, and $Zt2$ (= 150 ohm) is presumed as the phase arm to the tower underneath impedance. Also, the other parameters of this multistory model can be found in [36].

In this simulation, in order to prevent reflections, a line termination with 30 km length is added at each side.

Regarding the probabilistic nature of the lightning wave, a probabilistic evaluation based on a statistical approach similar to Monte Carlo simulation has been utilized. To create the main lightning parameters, each of these parameters (x) is approximated by a log-normal probability density function as follows [34]:

$$p(x) = \frac{1}{\sqrt{2\pi} \cdot \sigma_{\ln x} x} \cdot \exp \left\{ -\frac{1}{2} \cdot \left(\frac{\ln x - \ln \bar{x}}{\sigma_{\ln x}} \right)^2 \right\}, \quad (9)$$

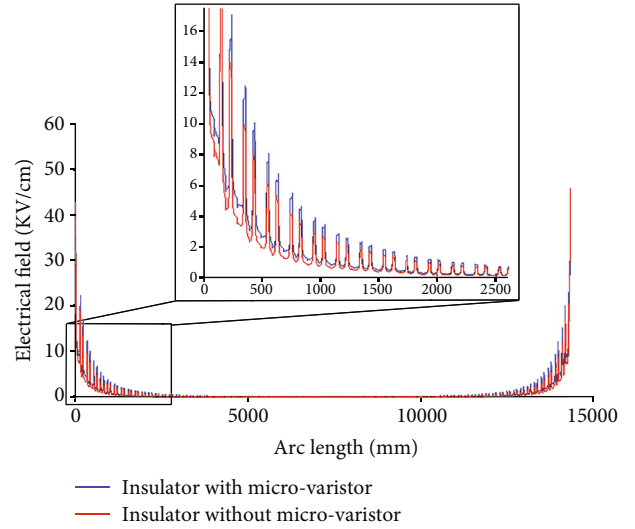


FIGURE 8: Electric field distribution in the surface of insulator with and without microvaristor.

where \bar{x} is the average of x and $\sigma_{\ln x}$ is the standard deviation.

The parameters of log-normal distribution are shown in Table 8.

The convergence of Monte Carlo simulation is obtained after 30000 runs. Figure 10 shows the distribution of randomly created variables for current magnitude and rise time.

5.4. *Computation of Outage Rate and Failure Risk.* By using the calculated CFO in previous section, the outage rate and the failure risk are calculated, and the impact of microvaristor on these parameters is evaluated. In following, formulizations of the aforementioned parameters have been presented.

The lightning performance of transmission line can be evaluated by LFOR and calculated as the following:

$$\text{LFOR} = N_g \times d \times \frac{F}{N}, \quad (10)$$

where $N_g = 1$ (flashes/km² year) is the ground flash density and $d = 1$ km and F are the number of flashovers in N runs. Further details can be found in [38].

TABLE 6: CFO values for different modelling of insulator.

Insulator models		CFO (kV)
Polluted insulator	Without microvaristor layers	1225.49
	With microvaristor-optimized layers	1413.70
Clean insulator	Without microvaristor layers	1495.87
	With microvaristor-optimized layers	1689.11

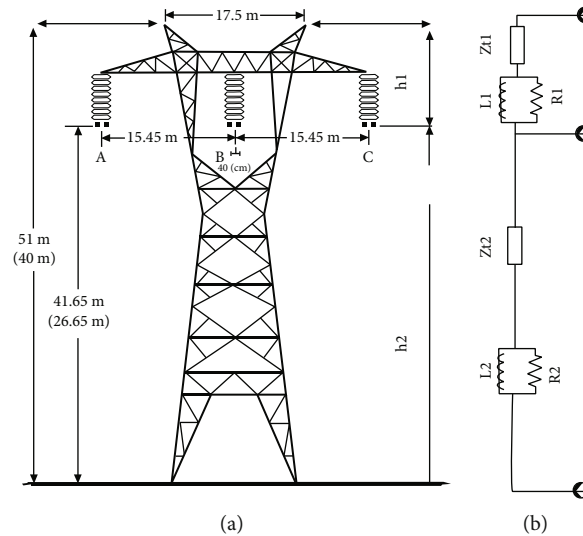


FIGURE 9: (a) Tower configuration and (b) multistory model of transmission tower layers.

TABLE 7: Line conductor characteristic.

Type	Diameter (cm)	Resistance (ohm/km)
Phase conductors	CURLEW	3.163
Shield wire	94S	1.26
		0.642

TABLE 8: Statistical parameters of lightning strokes [37].

Parameters	\bar{x}	$\sigma_{\ln x}$
I_p (KA)	31.1	0.48
t_f (μs)	3.83	0.55
t_p (μs)	77.5	0.58

The line outage cost is an important parameter in the lightning issues. The annual outage costs can be calculated as follows [39]:

$$C_{\text{outage}} = \text{LFOR} \cdot P_0(C_{\text{kWh}} t), \quad (11)$$

where P_0 (kW) is the outage power due to line trip-out, t (h) is the average of failure duration, and C_{kWh} is the average of annual cost of undelivered energy per kWh. In this paper, $P_0 = 100$ MW, $t = 60$ min, and $C_{\text{kWh}} = 0.06$ \$/kWh.

Also, the insulator failure risk can be obtained by the following expression [40]:

$$\text{F.R.} = \int_0^{\infty} f(V) \cdot P(V) \cdot dV, \quad (12)$$

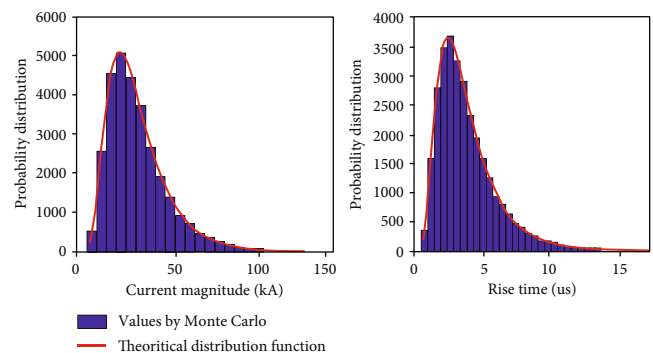


FIGURE 10: Distribution of randomly created variables of the first lightning stroke.

where $f(V)$ is the probability density function of over-voltage occurrences and $P(V)$ is the probability of disruptive discharge. The normal distribution function is considered for the $f(V)$ function:

$$f(V) = \frac{1}{\sigma_O \sqrt{2\pi}} \exp\left(-\frac{(V - V_O)^2}{2\sigma_O^2}\right). \quad (13)$$

TABLE 9: Outage rate and outage cost for different modelling of insulator.

Footing impedance (ohm)	Clean insulator				Polluted insulator			
	Without microvaristor CFO =1495.87 (kV)		With microvaristor CFO =1689.11 (kV)		Without microvaristor CFO =1225.49 (kV)		With microvaristor CFO =1413.70 (kV)	
	LFOR	C_{outage} (\$)	LFOR	C_{outage} (\$)	LFOR	C_{outage} (\$)	LFOR	C_{outage} (\$)
20	0.14	8.4	0.06	3.6	0.35	21	0.18	10.8
100	0.53	31.8	0.37	22.2	0.72	43.2	0.59	35.4
200	0.78	46.8	0.65	39	0.89	53.4	0.81	48.6

TABLE 10: Failure risk (F.R.) for different modelling of insulator.

Footing impedance (ohm)	Clean insulator		Polluted insulator	
	Without microvaristor CFO =1495.87 (kV)	With microvaristor CFO =1689.11 (kV)	Without microvaristor CFO =1225.49 (kV)	With microvaristor CFO =1413.70 (kV)
	F.R. (%)	F.R. (%)	F.R. (%)	F.R. (%)
20	0.135	0.076	0.242	0.159
100	0.296	0.193	0.436	0.328
200	0.405	0.294	0.481	0.449

The mean of over voltages (V_O) and standard deviation (σ_O) are achieved by running of Monte Carlo for 30000 times.

$P(V)$ function containing the value of CFO and standard deviation (σ_{in}) can also be calculated as follows:

$$P(V) = \frac{1}{\sigma_{in}\sqrt{2\pi}} \int_{-\infty}^V \exp\left(-\frac{(V-CFO)^2}{2\sigma_{in}^2}\right) dV. \quad (14)$$

5.5. Simulation Results and Discussion. According to the results of Table 6, evaluations are investigated in four different models: (i) model of insulator with ZnO microvaristor under clean surface conditions; (ii) model of insulator with ZnO microvaristor under contaminated surface conditions; (iii) model of insulator without ZnO microvaristor under clean surface conditions; (iv) model of insulator without ZnO microvaristor under contaminated surface conditions.

Table 9 presents LFOR and the outage cost for four different cases of the insulator by using Monte Carlo simulation with different footing resistance (R_f). The CFO values of the insulator are adopted from the results in Table 6. The failure risk of different insulators is calculated and summarized in Table 10.

Based on the obtained results, it can conclude that a microvaristor layer in the structure of the insulator can improve and change the flashover rate and the failure risk of insulator compared to the insulator without microvaristor. Also, it is obvious that the outage rate and risk are increased in the certain CFO value when footing impedance increment, which is the expected result.

Applying the insulator with microvaristor reduces the outage rate so that under the same circumstances, the outage rate of the insulator without microvaristor in the footing resistance is twice more than the outage rate of the insulator with microvaristor. The results reveal that using microvaristor not only optimizes the performance of the insulator but

also decreases the outage rate, outage expenses, and the risk. In other words, it enhances the system's reliability.

According to the obtained results, the use of microvaristor technology for optimizing the insulator performance has been evaluated positively.

6. Conclusion

This paper is aimed at investigating the effects of the microvaristor layer injection on the network, the outage rate, and other electrical parameters. Accordingly, through the analysis of the simulation results, the following conclusions were obtained.

The optimized microvaristor layers cause the decrement of the maximum electric field and the uniformity of the field distribution on the insulator surface, and the reduction of the maximum intensity of the field reduces the contamination deposition around the electrodes.

The dissipated power in the volume of the insulator decreases in the presence of microvaristor, which means a reduction in the temperature and heat on the insulator surface.

By changing the value of CFO, LFOR also changes; therefore, the number of outages and the costs related to it reduce.

Generally, according to the above results, the microvaristor layer prevents premature aging of composite insulators and increases the insulator lifetime. Also, it can also reduce the network outages, which means increasing the degree of reliability and decreasing the risk.

Data Availability

The original/processed data required to reproduce these findings cannot be shared at this time as the data also forms part of an ongoing study.

Conflicts of Interest

The authors declare that they have no conflicts of interest.

Acknowledgments

This work was supported by national funds through FCT (Fundação para a Ciência e a Tecnologia), under project UIDB/50021/2020. The authors want to acknowledge the support of Masoumeh Abdali.

References

- [1] B. Marungsri and W. Onchantuek, "Simulation of electric field and potential distributions on silicone rubber polymer insulators under contamination conditions using finite element method," *WSEAS Transactions on Power Systems*, vol. 3, no. 9, pp. 608–621, 2008.
- [2] F. Aouabed, A. Bayadi, and R. Boudissa, "Flashover voltage of silicone insulating surface covered by water droplets under AC voltage," *Electric Power Systems Research*, vol. 143, pp. 66–72, 2017.
- [3] R. Hackam, "Outdoor HV composite polymeric insulators," *IEEE Transactions on Dielectrics and Electrical Insulation*, vol. 6, no. 5, pp. 557–585, 1999.
- [4] R. Abd-Rahman, A. Haddad, N. Harid, and H. Griffiths, "Stress control on polymeric outdoor insulators using zinc oxide microvaristor composites," *IEEE Transactions on Dielectrics and Electrical Insulation*, vol. 19, no. 2, pp. 705–713, 2012.
- [5] M. R. Aghaebrahimi, R. Shariatinasab, and M. Ghayedi, "Optimal design of grading ring of surge arresters due to electric field distribution," in *2012 16th IEEE Mediterranean Electrotechnical Conference*, pp. 548–550, Yasmine Hammamet, Tunisia, March 2012.
- [6] M. Ghayedi and M. Jasinski, "Electric field distribution on zinc oxide pills in gapless surge arresters using finite element method and evolutionary optimization algorithms in HVDC systems," *Sustainability*, vol. 15, no. 10, pp. 1–13, 2023.
- [7] F. Aouabed, A. Bayadi, A. E. Rahmani, and R. Boudissa, "Finite element modelling of electric field and voltage distribution on a silicone insulating surface covered with water droplets," *IEEE Transactions on Dielectrics and Electrical Insulation*, vol. 25, no. 2, pp. 413–420, 2018.
- [8] R. Shariatinasab, S. Saghafi, M. Khorashadizadeh, and M. Ghayedi, "Probabilistic assessment of insulator failure under contaminated conditions," *IET Science, Measurement & Technology*, vol. 14, no. 5, pp. 557–563, 2020.
- [9] A. Naeini, E. A. Cherney, and S. H. Jayaram, "Temperature and electric field distributions along a form wound coil of an inverter-fed rotating machine with micro-varistor stress grading system," *IEEE Transactions on Dielectrics and Electrical Insulation*, vol. 27, no. 1, pp. 112–120, 2020.
- [10] Q. Shao, W. Sima, P. Sun, M. Yang, H. Xu, and Z. Yin, "A novel non-linear conductive ZnO micro-varistor/epoxy resin composite film for metallic particle deactivation in DC GIL," *IEEE Transactions on Dielectrics and Electrical Insulation*, vol. 27, no. 2, pp. 675–683, 2020.
- [11] H. Bishwakarma, R. Tyagi, N. Kumar, and A. K. Das, "Green synthesis of flower shape ZnO-GO nanocomposite through optimized discharge parameter and its efficiency in energy storage device," *Environmental Research*, vol. 218, article 115021, 2023.
- [12] I. Fofana, "50 years in the development of insulating liquids," *IEEE Electrical Insulation Magazine*, vol. 29, no. 5, pp. 13–25, 2013.
- [13] M. Rafiq, Y. Lv, and C. Li, "A review on properties, opportunities, and challenges of transformer oil-based nanofluids," *Journal of Nanomaterials*, vol. 2016, Article ID 8371560, 23 pages, 2016.
- [14] H. Duzkaya and A. Beroual, "Statistical analysis of ac dielectric strength of natural ester-based ZnO nanofluids," *Energies*, vol. 14, no. 1, p. 99, 2021.
- [15] J. Xie, J. Hu, J. He, Z. Guo, and Y. Yin, "Effect of silicone rubber polymer composites on nonuniform electric fields of rod-plane gaps," in *2013 Annual Report Conference on Electrical Insulation and Dielectric Phenomena*, Chenzhen, China, October 2013.
- [16] X. Zhao, P. Meng, J. Hu, Q. Li, and J. He, "Simulation and design of 500 kV DC cable terminal accessory based on ZnO varistor microsphere composites," *IEEE Transactions on Dielectrics and Electrical Insulation*, vol. 27, no. 1, pp. 10–16, 2020.
- [17] M. Pradhan, H. Grejjer, G. Eriksson, and M. Unge, "Functional behaviors of electric field grading composite materials," *IEEE Transactions on Dielectrics and Electrical Insulation*, vol. 23, no. 2, pp. 768–778, 2016.
- [18] Z. Huang, Z. Yuan, G. Sun, Y. Sun, J. Hu, and J. He, "Thickness effect on threshold electric field of ZnO microvaristors/silicone rubber composite with nonlinear conductivity," *Composites Part A: Applied Science and Manufacturing*, vol. 158, article 106969, 2022.
- [19] X. Zhang, M. Q. le, V. C. Nguyen et al., "Characterization of micro-ZnO/PDMS composite structured via dielectrophoresis - toward medical application," *Materials & Design*, vol. 208, article 109912, 2021.
- [20] X. Zhao, X. Yang, J. Hu et al., "Grading of electric field distribution of AC polymeric outdoor insulators using field grading material," *IEEE Transactions on Dielectrics and Electrical Insulation*, vol. 26, no. 4, pp. 1253–1260, 2019.
- [21] M. M. Touse and M. Ghassemi, "Combined geometrical techniques and applying nonlinear field dependent conductivity layers to address the high electric field stress issue in high voltage high-density wide bandgap power modules," *IEEE Transactions on Dielectrics and Electrical Insulation*, vol. 27, no. 1, pp. 305–313, 2020.
- [22] A. Shuhaimy and N. Hanani, *Sudy on non-linear grading material as stress control on polymeric outdoor insulator*, Doctoral dissertation, Faculty of Electrical and Electronic Engineering, Universiti Tun Hussein Onn Malaysia, 2014.
- [23] "Taban Niroo Co. 400KV TRANSMISSION SILICONE RUBBER INSULATORS," <http://taban-niroo.com/index.php/en/products/dpl-insulators/transmission-insulators/400-kv/item/141-dpl-400>.
- [24] H. Boulanouar, A. Bayadi, and A. Haddad, "Analysis of textured silicone rubber performance under contaminated conditions," *IET Science, Measurement & Technology*, vol. 13, no. 3, pp. 461–468, 2019.
- [25] C. G. Chand, R. Maity, K. Srinivasa Rao, N. P. Maity, and K. G. Sravani, "Electromechanical modelling and stress analysis of RF MEMS capacitive shunt switch," *Microsystem Technologies*, vol. 28, no. 9, pp. 2159–2167, 2022.
- [26] R. Maity, K. Gogoi, and N. P. Maity, "Micro-electro-mechanical-system based capacitive ultrasonic transducer as an

- efficient immersion sensor,” *Microsystem Technologies*, vol. 25, no. 12, pp. 4663–4670, 2019.
- [27] Z. Lei, B. Wu, S. Wu, Y. Nie, S. Cheng, and C. Zhang, “A material point-finite element (MPM-FEM) model for simulating three-dimensional soil-structure interactions with the hybrid contact method,” *Computers and Geotechnics*, vol. 152, article 105009, 2022.
- [28] B. Diban and G. Mazzanti, “The effect of temperature and stress coefficients of electrical conductivity on the life of HVDC extruded cable insulation subjected to type test conditions,” *IEEE Transactions on Dielectrics and Electrical Insulation*, vol. 27, no. 4, pp. 1313–1321, 2020.
- [29] C. Muniraj and S. Chandrasekar, “Finite element modeling for electric field and voltage distribution along the polluted polymeric insulator,” *World Journal of Modelling and Simulation*, vol. 8, no. 4, pp. 310–320, 2012.
- [30] Z. Zhan, J. Zhang, Y. Li, and H. Chung, “Adaptive particle swarm optimization,” *IEEE Transactions on Systems*, vol. 39, no. 6, pp. 1362–1381, 2009.
- [31] X. Zhang, X. Zhang, and Z. Wu, “Utility- and fairness-based spectrum allocation of cellular networks by an adaptive particle swarm optimization algorithm,” *IEEE Transactions on Emerging Topics in Computational Intelligence*, vol. 4, no. 1, pp. 42–50, 2020.
- [32] E. Kuffel, W. S. Zaengl, and J. Kuffel, “Electrostatic fields and field stress control,” in *High Voltage Engineering Fundamentals*, pp. 201–203, Butterworth-Heinemann, UK, 2nd edition, 2000.
- [33] S. Visacro, F. H. Silveira, and M. H. M. Vale, “Simplified representation of tower-footing electrodes for assessment of the lightning performance of transmission lines using EMTP-based platform,” in *The International Conference on Power Systems Transients (IPST2015)*, pp. 1–5, Cavtat, Croatia, June 2015.
- [34] J. A. Martinez and F. C. Aranda, “Parametric analysis of the lightning performance of overhead transmission lines using an electromagnetic transients program,” in *International Conference on Power Systems Transients-IPST*, pp. 1–6, New Orleans, USA, 2003.
- [35] A. R. Hileman, *Insulation coordination for power systems*, Marcel Dekker, New York, USA, 1999.
- [36] R. Shariatinasab and J. Gholinezhad, “The effect of grounding system modeling on lightning-related studies of transmission lines,” *Journal of Applied Research and Technology*, vol. 15, no. 6, pp. 545–554, 2017.
- [37] P. Chowdhuri, J. G. Anderson, W. A. Chisholm et al., “Parameters of lightning strokes: a review,” *IEEE Transactions on Power Delivery*, vol. 20, no. 1, pp. 346–358, 2005.
- [38] A. Shafaei, A. Gholami, and R. Shariatinasab, “Probabilistic evaluation of lightning performance of overhead transmission lines, considering non-vertical strokes,” *Scientia Iranica*, vol. 19, no. 3, pp. 812–819, 2012.
- [39] N. A. Katic and M. S. Savic, “Technical and economical optimisation of overhead power distribution line lightning protection,” *IEE Proceedings - Generation, Transmission and Distribution*, vol. 145, no. 3, pp. 239–244, 1998.
- [40] T. Dokic et al., “Risk assessment of a transmission line insulation breakdown due to lightning and severe weather,” in *2016 49th Hawaii International Conference on System Sciences (HICSS)*, pp. 2488–2497, Koloa, HI, USA, January 2016.